doi:10.3788/gzxb20164504.0412001

# 基于数字全息干涉术的液相扩散过程可视化

王骏[1,2],杨蓉[1],郑娇[1],赵建林[2]
(1 西安理工大学 机械与精密仪器工程学院,西安 710048)
(2 西北工业大学 理学院 陕西省光信息技术重点实验室 空间应用物理与化学教育部重点实验室,西安 710072)

**摘 要**:提出了利用数字全息干涉术可视化观测液相扩散过程.实验中,采用马赫-曾德干涉仪光路记录乙醇与水之间两相扩散过程的多幅数字全息图;再通过数值再现不同扩散状态的波前相位分布,获得液体中的摩尔浓度分布;最后,根据菲克定律获得两相流扩散系数.结果表明:利用数字全息干涉术可实现对液相扩散传质过程的快速、实时及高精度测量;该方法还具有可实现远程监控、拥有大量微观数据的优点;此外,采用文中全息干涉光路结合波分与角分复用技术可实现多相流扩散系数的测量,为获得溶液中非线性变化特征参量提供了有效技术手段.

**关键词**:数字全息;相干成像;数字全息干涉术;数字图象处理;液相扩散过程;扩散系数
**中图分类号**:TN26 **文献标识码**:A **文章编号**:1004-4213(2016)04-0412001-7

# Visualized Measurement of the Liquid Phase Diffusion by Using Digital Holographic Interferometry

WANG Jun[1,2], YANG Rong[1], ZHENG Jiao[1], ZHAO Jian-lin[2]
(1 *School of Mechanical and Precision Instrument Engineering, Xi'an University of Technology, Xi'an* 710048, *China*)
(2 *Shaanxi Key Laboratory of Optical Information Technology and the Key Laboratory of Space Applied Physics and Chemistry, Ministry of Education, School of Science, Northwestern Polytechnical University, Xi'an* 710072, *China*)

**Abstract**: Liquid phase diffusion is a high energy consumption process in chemical production. With the rapid development of the chemical technology based on liquid phase diffusion, especially in some emerging fields such as biomedicine and environmental science, the microcosmic study on the liquid phase diffusion is becoming more and more important. By applying the digital holographic interferometry, a diffusion process in liquid phase of pure ethanol and water was observed. After recording the digital hologram by a Mach-Zehnder interferometer and reconstructing digital hologram of object beam by the gray scale analysis, the phase variation of object wavefront in the diffusion process at different times and the curves of refractive index change in the diffusion area were both acquired. The result shows that by applying the digital holographic interferometry, a fast, real time and high-accuracy diffusion can be realized. Moreover, this method can be used to realize a remote visual monitoring. In addition, this method combining with wavelength and angular multiplexing techniques can be applied to obtain nonlinear characteristics parameters in multiple-phase diffusion measurements.

**Key words**: Digital holography; Coherence imaging; Digital holographic interferometry; Digital image processing; Liquid phase diffusion; Diffusion coefficient
**OCIS Codes**: 120.2880; 090.1995; 110.1650; 100.2000

**Foundation item**: The National Natural Science Foundation of China (Nos. 61127011, 61575159), the China Postdoctoral Science Foundation (No. 2015M570846) and the Department of Education Fund in Shaanxi Province of China (No. 15JK1529)
**First author**: WANG Jun(1979— ), male, lecturer, Ph. D. degree, mainly focuses on digital holography. Email:wangjun790102@xaut.edu.cn
**Contact author**: ZHAO Jian-lin(1958— ), male, professor, Ph. D. degree, mainly focuses on digital optical information processing and digital holography. Email:jlzhao@nwpu.edu.cn
**Received**: Oct. 10, 2015; **Accepted**: Feb. 1, 2016

## 0 Introduction

Liquid phase diffusion is a high energy consumption process in chemical production. With the rapid development of the chemical technology based on liquid phase diffusion, especially in some emerging fields such as biomedicine and environmental science[1-2], the microcosmic study on the liquid phase diffusion is becoming more and more important. Since last century early, many diffusion models have been proposed to enhance the mass transfer efficiency and explain the two-phase interfacial mass transfer accurately in microcosm [3-5]. At present, experimental methods to measure the liquid phase diffusion mainly include Optical Holographic Interferometry (OHI)[6-7], diaphragm cell[8] and Nuclear Magnetic Resonance (NMR)[9], *etc*. The diffusion data are obtained by analyzing the holographic interference fringes reconstructed from the recorded hologram in the method of OHI. In diaphragm cell method, the solutions with different consistency pass through the micropore film and diffusion, thus the consistency change in both sides can be measured to obtain the diffusion coefficient. NMR method gets the diffusion coefficient by the medium atomic moment rotation in magnetic disturbances. Gabelmann-Gray[6] and Jean[7] *et al*. applied OHI to determine the diffusion coefficient of sucrose-water or gypsum-water system successively. Singh *et al*[8] used a diaphragm cell method to measure the diffusion coefficient of PbBr2-AgBr system. Claudio *et al*[9] studied the two phase media diffusion of PVdF-HFP and $LiN(C_2F_5SO_2)_2$ with NMR method. But in the diaphragm cell method, the main medium flow will be brought into the diffusion process and the remained shell will exist in both sides of the film which affect the measurement accuracy. NMR has a rapid measurement rate and a high accuracy, but both nuclear magnetic moment and angular momentum of the media molecules are required to be non-vanishing which limits its application fields. The absolute value of the diffusion data can be acquired directly with a high accuracy in OHI, but the holographic plate for recording hologram needs a complicated wet chemical processing and using this method one can only obtain limited diffusion data at a certain time.

Different from OHI, Digital Holographic Interferometry (DHI) uses a Charge Coupled Device (CCD) or the Complementary Metal-Oxide-Semiconductor (CMOS) transistors to record the hologram and numerically reconstructs the holographic interferogram by computer, which leaves out the complicated wet chemical processing of the holographic plate and thus is considered as a new potential tool for measuring flow field or phase diffusion. Sun *et al* [10] realized the visual measurement of the Karman Vortex Street in water flow field by using DHI and got its dynamic distribution. Gopalan *et al*[11] observed the decomposition of the petrol under dispersant employing digital holographic microscopy. Hossain *et al*[12] applied digital lensless Fourier transform holography to study the temperature distribution of the layered free thermal convection field in water and analyzed its temperature variation. In this paper, we present a realization method of the dynamic display of the liquid phase diffusion and the measurement of the diffusion coefficient based on DHI. Analyzing the shapes of interference fringes, to get diffusion coefficient in OHI, are avoided by obtaining the phase distribution in DHI. The hologram is digitally recorded which is conducive for a long-distance storage, transmission and reconstruction, so it's also useful in the remote visual monitoring process of liquid phase diffusion. In addition, this method combining with wavelength and angular multiplexing techniques can be applied to obtain nonlinear characteristics parameters in multiple-phase diffusion measurements.

## 1 Principles

In the transparent two-phase flow media, the refractive index distribution in interdiffusion region changes due to the diffusion between two media and this will affect the phase distribution of the wavefront of the object beam passing through the media. That is to say, the phase distribution varies with the refractive index distribution in the interdiffusion process. In order to record the phase distribution, a reference beam is introduced to interfere with this object beam in different states to form a series of holograms. These holograms are separately recorded by a CCD and the corresponding reconstructed complex amplitude distributions of the object beams bring the refractive index distribution information in diffusion region. The phase change can be calculated by comparing with the complex amplitude distributions. Furthermore, the refractive index change under different states can be obtained.

Assuming that the intensity distribution of two recorded holograms in interdiffusion states is given by

$$I_i(x,y)=|U_i(x,y)+R(x,y)|^2=(r_0^2+u_0^2)+u_0r_0\cdot\exp[\mathrm{j}(\varphi_i-\varphi_r)]+u_0r_0\exp[-\mathrm{j}(\varphi_i-\varphi_r)] \quad (1)$$

where, $U_i(x,y)=u_0(x,y)\exp[\mathrm{j}\varphi_i(x,y)]$ and $R(x,y)=r_0(x,y)\exp[\mathrm{j}\varphi_r(x,y)]$ describe the complex amplitude of the object and reference beams in the recording plane, $\varphi_i(x,y)$ and $\varphi_r(x,y)$ depict the phase

distributions of the corresponding wavefronts, and $i=0, 1, 2, \cdots$ represent the initial and different diffusion states, respectively. Similar to the optical double-exposure holographic interferometry, we can add up the intensity (gray) distributions of two holograms recorded in initial and a certain diffusion states to get a composed digital hologram, whose intensity distribution will be given by

$$I_{ci}(x,y)=I_0(x,y)+I_i(x,y)=2(r_0^2+u_0^2)+u_0 r_0\exp[\mathrm{j}(\varphi_0-\varphi_r)]+u_0 r_0\exp[-\mathrm{j}(\varphi_0-\varphi_r)]+u_0 r_0\exp[\mathrm{j}(\varphi_i-\varphi_r)]+u_0 r_0\exp[-\mathrm{j}(\varphi_i-\varphi_r)] \quad (2)$$

The holographic interferogram of the two reconstructed object beams in diffusion states can be obtained by numerically simulating the diffraction of the composed digital hologram, of which the intensity distribution is expressed by

$$I_{hi}(x,y)=I_{h0}(x,y)\cos^2\left[\frac{\Delta\varphi_i(x,y)}{2}\right] \quad (3)$$

where, $I_{h0}(x,y)\propto 4u_0^2(x,y)r_0^4(x,y)$, $\Delta\varphi_i(x,y)=\varphi_i(x,y)-\varphi_0(x,y)$. Eq. (3) shows that the intensity envelope of the reconstructed holographic interferogram forms a cosine-square distribution modulated by relative phase change $\Delta\varphi_i$ depending on the optical path difference of the object beam. Assuming that the index changes only along at the transverse direction and the medium thickness is uniform, the relationship between refractive index and relative phase change $\Delta\varphi_i$ can be expressed by

$$n(x,y)=f[\Delta\varphi(x,y)]=n_0\pm\frac{\Delta\varphi(x,y)\lambda}{2\pi L} \quad (4)$$

where, $n_0$ is the initial index, $\lambda$ is the beam wavelength, $L$ is the thickness of solution in the container, and $\Delta\varphi(x,y)$ is the phase change between initial and current states of the solution.

According to the Lorentz-Lorenz formula, the index $n$ of binary solution satisfies following the relation [13]

$$\frac{n^2(x,y)-1}{n^2(x,y)+2}=\sum_{i=1}^{2}\psi_i\frac{n_i^2(x,y)-1}{n_i^2(x,y)+2} \quad (5)$$

where, $\psi_i$ and $n_i(x,y)$ are the volume fraction and index of the respective components in the solution, respectively. Eq. (5) can be applied if the solution is dilute. In addition, the indices of solute and solvent are nearly the same.

The relationship between the index change and the concentration variation of the respective components, which is also related with the temperature, can be expressed as [14]

$$\Delta n_i(x,y)=\left[\frac{\partial n_{is}}{\partial T}\right]_C[T_t(x,y)-T_0(x,y)]+\left[\frac{\partial n_{is}}{\partial c_i}\right]_T[c_{it}(x,y)-c_{i0}(x,y)] \quad (6)$$

where, $c_{i0}(x,y)$ and $T_0(x,y)$ are the concentration and temperature at the initial time, and $c_{it}(x,y)$ and $T_t(x,y)$ are the concentration and temperature at time $t$, $(\partial n_{is}/\partial T)_c$ and $(\partial n_{is}/\partial c_i)_T$ are the dependence of the index on temperature and concentration, respectively. Under the condition of constant temperature, Eq. (3) can be simplified as

$$\Delta n_i(x,y)=\left[\frac{\partial n_{is}}{\partial c_i}\right]_T[c_{it}(x,y)-c_{i0}(x,y)] \quad (7)$$

The relationship between the index and the concentration of the respective components can be expressed as

$$c_{it}(x,y)=c_{i0}(x,y)+[n_i(x,y)-n_{i0}(x,y)]/\left[\frac{\partial n_{is}}{\partial c_i}\right]_T \quad (8)$$

where, $n_{i0}(x,y)$ is the initial index of the respective components, $c_{i0}(x,y)$ and $c_{it}(x,y)$ are the concentration of the respective components at initial time and at different time, respectively. $[\partial n_{is}/\partial c_i]_T$ is the dependence of solution index on the concentration at the temperature $T$. The solutions with different concentrations correspond to different indices. By measuring the relationship between index and concentration using V-prism refractometer, the $[\partial n_{is}/\partial c_i]_T$ can be obtained. Consequently the concentrations of solution at different time can be obtained by Eq. (8). So the solution concentration in corresponding states can be calculated out according to the relationship between the index $n_i$ and the liquid concentration. Furthermore, we can get the diffusion coefficient based on the Fick's law of diffusion. It can be expressed as

$$\frac{c_1-c_{10}}{c_{1\infty}-c_{10}}=\mathrm{erf}\frac{z}{\sqrt{4Dt}} \quad (9)$$

where, $D$ is two-phase diffusion coefficient; $c_1$ describes the molar concentration at time $t$; $c_{10}$ is the initial mole concentration above the interface; $c_{1\infty}$ is the initial mole concentration below the interface; $z$ and $t$ are the diffusion layer position and time, respectively; symbol "erf" is the Gaussian error function.

The gray scale of a pixel of the phase change distribution map is 256, so the corresponding precision of the phase change is $2\pi/256$. According to Eq. (4), the precision of index change can be expressed as follows

$$\delta_{\Delta n}=\frac{\lambda}{256L} \quad (10)$$

Then, combining Eqs. (8) and (10), the measurement accuracy of concentration can be calculated. Considering the effect of the zoom multiple of the optical system, the size resolution that can be expressed by the size of the analyte imaged in a single pixel will be given by

$$\delta=\Gamma\frac{S}{M} \quad (11)$$

where, $\Gamma$ is the zoom multiple of optical system, $S$ and $M$ are the dimension and pixel number of recording medium in vertical direction, respectively. According to Eq. (11), the measurement accuracy can be improved by increasing the zoom multiple of optical system or/and the pixel number in unit length.

Therefore, the dynamic display and measurement of the phase diffusion in two-phase liquid flow system based on DHI is actually the measurement of the corresponding phase change of the illumination object beam.

## 2 Experimental setup

Fig. 1 shows the experimental setup, which adopts image plane holography to record the digital holograms of the samples. The digital hologram in the diffusion area is recorded applying a Mach-Zehnder interferometer. A light beam from a fiber-coupled laser ($\lambda$=532 nm) is divided into two parts by a 1×2 fiber coupler. One part serves as the object beam, while the other part acts as the reference beam. The collimated object beam obtained after passing through the lens $L_1$ is incident orthogonally on the quartz container with dimension of 50mm×50mm×100mm and illuminates the solution in the container. A 4$f$ system (lens $L_2$ and $L_3$) is introduced in the object beam path, to reduce beam size comparable to the CCD target placed opposite to the beam splitter BS. The reference beam is collimated by lens $L_4$ and interferes with the object beam at the CCD target ($1625_W \times 1235_H$ pixels with pixel size of 7.4 μm × 7.4 μm), after reflection through the BS. The neutral filter F is used to attenuate the beam intensity.

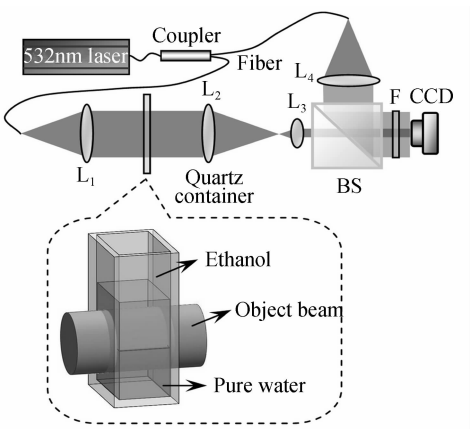


Fig. 1 Fiber-based digital holographic experimental setup for the record of digital holograms of two-phase flow diffusion

In traditional DHI, pinholes are generally used to filter out the high spatial frequency noises. Considering the better performance in filtering the noises, which is relative to pinhole, the fiber coupler made of 460HP fiber with core diameter of 4 μm is employed in the experiment to replace two pinholes, two beam expanders and one beam splitter, thus resulting in a relatively simplified setup. Moreover, it also helps to relax the requirement of the laser performance parameters *e. g.* coherence length and beam uniformity.

The samples in the quartz container are 99.7% ethanol and pure water. In order to prevent convection in the diffusion, high density liquid is put in the bottom of experimental quartz container. The ethanol with less specific gravity is put first to the experimental cell, and then kept still for 10 minutes. Afterward, pure water with more specific gravity is injected slowly from the bottom of experimental cell to avoid disturbance in the interface. After the injection, adhesive tape is used to seal vent on top of the experimental cell to avoid the volatilization of ethanol in the process of measure thus affect measurement results.

In our experiment, the digital hologram is recorded by the CCD once every $\Delta t$ time, and the $m$($m$=1, 2, 3, …, $M$) hologram and the first one in initial state are numerical reconstructed with DHI. So the relative phase change $\Delta\varphi_m$ of the object beam at $t=m\Delta t$ time can be calculated and the refractive index distribution under different states in the liquid phase diffusion process can be obtained according to the initial medium refractive index.

## 3 Results and analysis

In the process of two-phase flow diffusion for one hour, one hologram is recorded after every 30s time interval. Fig. 2(a) shows the digital hologram of the diffusion field at 60$^{th}$ min. The upper fringes in Fig. 2(b) show the index variation caused by water diffusing through ethanol. The middle black area originates from

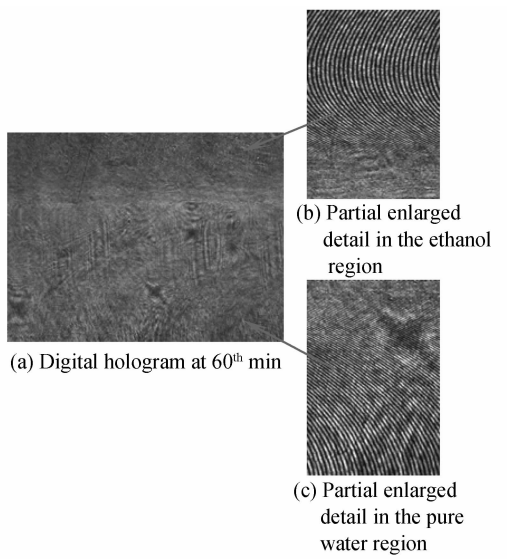


Fig. 2 Digital hologram of the diffusion field and partial enlarged detail

class lens effect which is formed by surface tension at two liquid interfaces. The lower part in Fig. 2(c) shows index change caused by diffusing from ethanol to water. In the reported literature[15], the diffusion coefficient is obtained by studying the change in the fringe pattern the process of mass transfer. That is to say, the curvature position, direction and degree of interference fringe in the interdiffusion region need to be measured. Because of the differences between the curvature degrees of interference fringes, the measurement precision of diffusion coefficient is low. So, the average of wavefront phases in the same horizontal plane will be calculated. Putting the average value into Eq. (4), the refractive index will be obtained with high accuracy.

In the experiment, by numerically reconstructing the object waves from the holograms at initial state and the mid-states, we obtain the corresponding phase distributions of the reconstructed object waves. The wrapped phase maps representing the distribution of the concentration fields are obtained by subtracting the phase distribution of the initial state from that of the mid-states. Figs. 3(a～f) show a sequence of the two-dimensional wrapped phase maps at $10^{th}$ min, $20^{th}$ min, $30^{th}$ min, $40^{th}$ min, $50^{th}$ min and $60^{th}$ min, respectively. It can be seen that the fringes appear parallel to the diffusion interface.

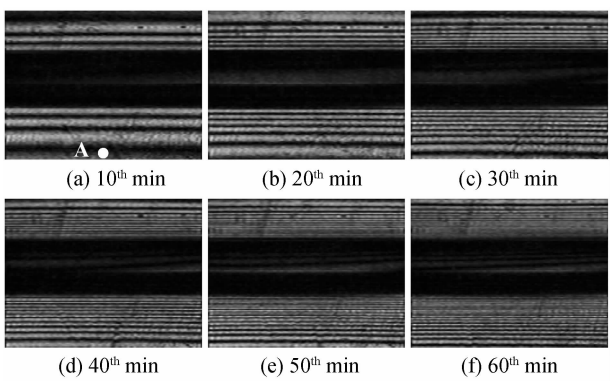


Fig. 3 Digital holographic interferometry in diffusion region at different time

We take point A on the bottom of experimental quartz container in Fig. 3(a) as reference to analyze the phase change $\Delta\varphi$. According to Eqs. (1)～(3) and variation of the fringes and grayscale in the Fig. 3, the phase change of wavefront in the diffusion area of a certain time can be worked out, as shown in Fig. 4. The curves in Fig. 4 represent the phase change of wavefront in the water and ethanol area, respectively. The ordinate is $\Delta\varphi$, and the abscissa is diffusion depth (representing pixels in the vertical direction of diffusion area). Each value on the ordinate is the average of wavefront phases in the same horizontal plane. We can find out that $\Delta\varphi$ increases with the time. The distance between each two adjacent curves represents the translation distance of the diffusion interface during the corresponding time interval.

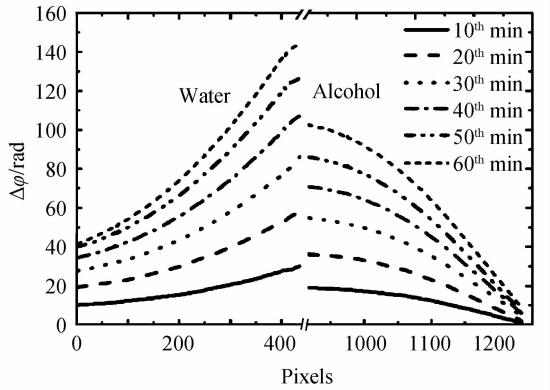


Fig. 4 Phase change of wavefront in the water and ethanol area at different time

At normal temperature and pressure, the refractive index of water and ethanol are 1.33 and 1.36 to 532 nm respectively. By stacking the index change in diffusion region of water and ethanol at different time and the initial refractive index, the refractive index of two media at different time is shown in Fig. 4, in which the ordinate presents refractive index $n$ and abscissa presents diffusion depth.

After the interdiffusion at 60 minutes, an ethanol-water solution layer is formed near the diffusion region. From Fig. 4, we can get that the index of the solution layer in water area increases with time, while the index of the solution layer in the ethanol area decreases with time. With diffusion going on, the index of solution eventually reaches a balance and the two refractive index distribution curves join together. This result is in accordance with the related study[16] which has already been published.

Fick diffusion coefficient includes two influence factors. One is MS diffusion coefficient, which express the frictional force at the relative motion of diffusion molecular. Because of a smaller variation of its value, MS diffusion coefficient can be ignored. The other is the influence of thermodynamics in the non-ideal state. Its value is expressed by thermodynamic factor, changing with non-ideal level. According to Eqs. (8) and (9), we obtain the diffusion coefficients of ethanol-water, as shown in Table 1. The $c_{ethanol}$ and $c_{water}$ are the molar concentrations of ethanol and water, respectively. In Fig. 3, the fringe variation between two adjacent states decreases gradually. It shows that the phase change decreases with the diffusion by considering the same area and diffusion time. The relationship among the phase change, index, concentration and diffusion coefficient reveals that the diffusion coefficient decreases with the diffusion time,

which is consistent with the hydrodynamic theory, and is also in accord with the relation between molecular frictional resistance and diffusion coefficient. Thus, with the increase of the solvent concentration in solution, frictional resistance among molecules increases and the diffusion coefficient decreases.

**Table 1 Diffusion coefficients of ethanol-water at room temperature and pressure**

| $c_{ethanol}$ | $c_{water}$ | $10^6 D/(m^2\ s^{-1})$ |
|---|---|---|
| 0.0 | 1.0 | 0.1 |
| 0.1 | 0.9 | −2.4 |
| 0.2 | 0.8 | −4.5 |

In Fig. 5, the spacing of index curve of adjacent time decreases gradually, which shows that the index change decreases with diffusion in the same area and at the same diffusion time (10 minutes). According to the relationship among index, concentration and diffusion coefficient, we can get the diffusion coefficient decreasing with the diffusion. This is in accordance with the result of the paper that diffusion coefficient decreases with the increase of vitamin C concentration in water when vitamin C and water interdiffusing, and is also in accordance with the relation between molecular friction resistance and diffusion coefficient. That is to say, with the increase of the consistency of the solute in solution, frictional resistance among molecules increases which causes decreasing of diffusion coefficient.

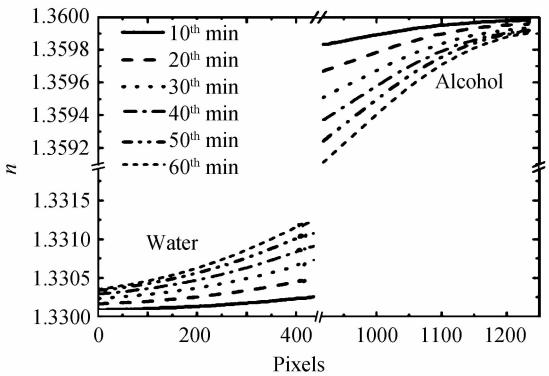


Fig. 5 Index change in the water and ethanol area at different time

## 4 Conclusion

By making use of DHI, the diffusion in ethanol-water system is dynamiclly measured for one hour, and digital hologram is recorded every 30 seconds. The curve of wavefront phase change and refractive index change in the diffusion area is acquired. The results show that the refractive index of two mediums is gradually same with the diffusion time. The refractive index change and diffusion coefficient decrease gradually with diffusing in the same area and at the same diffusion time. The experimental results are consistent with reports on the related paper. Applying DHI to study the phase change in two-phase flow has the advantages of fast, real-time, high measure accuracy, monitoring and *etc*. Because of the above advantages, DHI is presented to improve the accuracy of diffusion coefficient. The applications of DHI will be expanded. In this paper, considering the aberration characteristics of the optical system and according to Eq. (10), the measurement accuracy can achieve $10^{-6}$ orders of magnitude. In addition, the temporal resolution of digital holographic system is determined by the sampling frequency of the recording medium. At present, the sampling frequency of a high-speed camera can be the million frames per second. By increasing the sampling frequency of holograms, the diffusion process can be subdivided. The measurement accuracy can be improved. Through properly adjusting light way of experiment, it can also visually measure appearance and evolution process of multi-phase flow.

**References**

[1] WON S H, VELOO P S, DOOLEY S, *et al*. Predicting the global combustion behaviors of petroleum-derived and alternative jet fuels by simple fuel property measurements[J]. *Fuel*, 2016, **168**: 34-46.

[2] PETRUSHENKO S I, DUKAROV S V, SUKHOV V N. Formation and thermal stability of liquid phase in layered film systems[J]. *Vacuum*, 2015, **122**: 208-214.

[3] XIE R L, VOROBEV A. On the phase-field modelling of a miscible liquid/liquid boundary[J]. *Journal of Colloid and Interface Science*, 2016, **464**: 48-58.

[4] MICHALIS V K, MOULTOS O A, TSIMPANOGIANNIS I N, *et al*. Molecular dynamics simulations of the diffusion coefficients of light n-alkanes in water over a wide range of temperature and pressure[J]. *Fluid Phase Equilibria*, 2016, **407**: 236-242.

[5] LUO Hui, XIAO Shi-fang, WANG Sheng-jie, *et al*. Molecular dynamics simulation of diffusion and viscosity of liquid lithium fluoride[J]. *Computational Materials Science*, 2016, **111**: 203-208.

[6] GRAY L G, FENICHEL H. Holographic interferometric study of liquid diffusion[J]. *Applied Optics*, 1979, **18**(3): 343-345.

[7] COLOMBANI J, BERT J. Holographic interferometry study of the dissolution and diffusion of gypsum in water[J]. *Geochimica Et Cosmochimica Acta*, 2007, **71**(8): 1913-1920.

[8] SINGH N B, GLICKSMAN M E, CORIELL S R, *et al*. Measurement of diffusion coefficient using a diaphragm cell: PbBr2-AgBr system[J]. *Journal of Crystal Growth*, 1996, **167**(1-2): 107-110.

[9] CAPIGLIA C, SAITO Y, KATAOKA H, *et al*. Structure and transport properties of polymer gel electrolytes based on PVdF-HFP and LiN(C2F5SO2)2[J]. *Solid State Ionics*, 2000, **131**(3-4): 291-299.

[10] SUN Wei-wei, ZHAO Jian-lin, DI Jiang-lei, *et al*. Real-time visualization of Karman vortex street in water flow field by using digital holography[J]. *Optics Express*, 2009, **17**(22): 20342-20348.

[11] GOPALAN B, KATZ J. Turbulent shearing of crude oil mixed with dispersants generates long microthreads and

microdroplets[J]. *Physical Review Letters*, 2010, **104**(5): 054501.

[12] HOSSAIN M M, SHAKHER C. Temperature measurement in laminar free convective flow using digital holography[J]. *Applied Optics*, 2009, **48**(10): 1869-1877.

[13] HELLE W. Remarks on refractive index mixture rules[J]. *Journal of Chemical Physics*, 1965, **69**: 1123-1129.

[14] ZHANG Yan-yan, ZHAO Jian-lin, DI Jiang-lei, *et al*. Real-time monitoring of the solution concentration variation during the crystallization process of protein-lysozyme by using digital holographic interferometry[J]. *Optics. Express*, 2012, **20**: 18415-18421.

[15] ARUN A, VANI K C, SHOMA M, *et al*. Diffusion studies in liquids by multiple beam interferometer[J]. *Optics and Laser Technology*, 2002, **34**: 45-49.

[16] ZHAO Chang-wei, LI Ji-ding, MA Pei-sheng. Diffusion studies in liquids by holographic interferometry[J]. *Optics and Laser Technology*, 2006, **38**(8): 658-662.